

# PCCP

Accepted Manuscript



This is an *Accepted Manuscript*, which has been through the Royal Society of Chemistry peer review process and has been accepted for publication.

*Accepted Manuscripts* are published online shortly after acceptance, before technical editing, formatting and proof reading. Using this free service, authors can make their results available to the community, in citable form, before we publish the edited article. We will replace this *Accepted Manuscript* with the edited and formatted *Advance Article* as soon as it is available.

You can find more information about *Accepted Manuscripts* in the [Information for Authors](#).

Please note that technical editing may introduce minor changes to the text and/or graphics, which may alter content. The journal's standard [Terms & Conditions](#) and the [Ethical guidelines](#) still apply. In no event shall the Royal Society of Chemistry be held responsible for any errors or omissions in this *Accepted Manuscript* or any consequences arising from the use of any information it contains.

Cite this: DOI: 10.1039/c0xx00000x

www.rsc.org/xxxxxx

PAPER

# Efficacy of Titanium doped-Indium Tin Oxide (Ti/TiO<sub>2</sub>-ITO) Films in Rapid Oxygen Generation under Photocatalysis and their Suitability for Bio-medical Application

A. Subrahmanyam,<sup>a</sup> A. Rajakumar,<sup>b\*</sup> Md. Rakibuddin,<sup>b</sup> T. Paul Ramesh,<sup>c</sup> M. Raveendra Kiran,<sup>d</sup> D. Shankari,<sup>a</sup> K. Chandrasekhar<sup>c</sup>

Received (in XXX, XXX) Xth XXXXXXXXXX 20XX, Accepted Xth XXXXXXXXXX 20XX

DOI: 10.1039/b000000

The present work details about the photocatalytic properties of controlled titanium doped indium tin oxide (Ti/TiO<sub>2</sub>-ITO) composite thin films prepared by DC magnetron sputtering and its applicability in developing a bio-medical lung assistive device. The catalytic films of various thicknesses (namely, C<sub>1</sub>, C<sub>2</sub>, C<sub>3</sub> and C<sub>4</sub>) were characterized using surface imaging (SEM), X-ray analyses (XRD and EDX), and Raman studies. The optical band gaps of the prepared films are ~ 3.72-3.77 eV. Photocatalytic efficiencies of the film catalysts were investigated with a help of a model organic molecule (Rhodamine B dye). The overall photodegradation capacity of the films was found to be slow in kinetics, and the catalyst C<sub>1</sub> was identified to have better degradation efficiency (RhB 5 ppm, at pH 6.5) in 5 h under irradiation at 254 nm. The speciality of the composite films is their oxygen accumulation capacity and unique electron-hole pair separation ability. Investigations on oxygen species revealed the formation of superoxide radicals in aqueous system (pH 6.5). The prepared films has TiO<sub>2</sub> in anatase phase in the surfaces, and possess desired photocatalytic efficiency, compatibility to heme system (does not involve harmful hydroxyl radical production), and appreciable reusability. Especially, the thin films have significant ability for mobilization of oxygen rapidly and continuously in the aqueous medium under the irradiation condition. Hence, these films can be a suitable choice for the photo-aided lung assistive design under development.

## 1. Introduction

Semiconductor and their doped composites have gained tremendous attention in recent decades due to their potential applications in solar energy harvesting, sensors, catalysis, superconducting devices and fuel cells.<sup>1-4</sup> Splitting of water into oxygen, and hydrogen is a well-established phenomenon of photocatalysis. There are several applications of the oxidative photocatalytic phenomena employed in environmental cleaning, especially in water treatment.<sup>5-13</sup> Our laboratory has been working on the development photocatalytic lung-assist device (or artificial lungs): a new and emerging bio-medical engineering application. One of the fundamental and primary functions of lungs, as is well known, is to oxygenate the blood. The oxygen binding proteins (haemoglobin and myoglobin) contain protoporphyrin IX (heme) as an essential prosthetic centre.<sup>14</sup> Oxygen is carried and transported by the haemoglobin in the red blood cells to the tissues for necessary metabolism. In the basic working of natural lungs, there is a membrane (in the alveoli) involved, which facilitates the gas diffusion (i.e., oxygen binding to blood and release of carbon dioxide from blood) from air into the red blood cells (haemoglobin: a complex protein that binds oxygen and carbon dioxide). The diffusion process is basically

controlled by the partial pressures of gases in the blood. Blood consists of red cells, white cells, platelets and plasma. Plasma is the relatively clear, yellow tinted solutions consisting of water (92+ %), sugar, fat, protein and salts. Normally, 55% of blood's volume is made up of plasma. Plasma is very similar to normal saline. The basic principle of the proposed lung-assist device is to photocatalyse the water/ plasma within the blood so that oxygen is produced in-situ right close to red blood cells. This is our hypothetical concept, and it is new. At present, the existing lung-assist devices employ the gas diffusion mechanisms with the help of artificial membranes or fibers to oxygenate blood (there are several limitations for the membrane oxygenators for long term usage). We have conducted several experiments of photocatalysis to produce oxygen in human blood and the results clearly indicate that the concept is viable and workable,<sup>15,16</sup> the human blood is observed to withstand and retain all the basic properties towards the UV exposure and photocatalytic process under our specified experimental conditions. The main requirements for this bio-medical application are (i) the photocatalysts being used should be bio and hemo compatible, (ii) the oxidative intermediates (like the hydroxyl radicals and singlet oxygen, etc.) produced during the photocatalytic process are detrimental for the proposed

application and (iii) the change in pH due to photocatalytic process in the blood should always lie within a very narrow range  $\sim 0.1$  (the pH of human blood should be within 7.35 to 7.45).

From literature, the Titanium dioxide ( $\text{TiO}_2$ ) in mixed phase of rutile and anatase is known as effective photocatalyst.<sup>17</sup> When metals were doped into titania, the photocatalytic efficiency was reported to be enhanced.<sup>18</sup> Our earlier results showed that tin doped indium oxide (ITO)<sup>19</sup> and titanium doped ITO thin films are proficient photocatalysts, and they are found reported to be bio-compatible. The main results on the photocatalytic oxygenation of human blood are (i) the mean increase in the percentage of saturation oxygen in blood ( $\text{SaO}_2$ ) is  $5.94 \pm 0.80$ , and an average increase in pH in test  $0.18 \pm 0.07$ , (for a total time of 300 minutes). Preliminary results of blood experiments conducted with  $\text{TiO}_2$  incorporated ITO photocatalyst have been reported<sup>15-16</sup> and are positive and encouraging in nature. Number of experiments conducted in our lab provided a lead that, when  $\text{TiO}_2$  thickness exceeding 150 nm on ITO/metal surface was providing undesired catalysis on biological samples. This is due to the production of rapidly reactive hydroxyl radicals as in the case like pure  $\text{TiO}_2$  slurry irradiated under strong UV light. A controlled thick of  $\text{TiO}_2$  would be preferential for milder catalytic reactions. More detailed results on human blood are being communicated to a medical journal as per biomedical protocol.

The present project is aimed at evaluating the photocatalytic efficiency of the controlled thickness of Titanium doped ITO ( $\text{TiO}_2/\text{Ti:ITO}$ ) films. These specific purpose catalytic composite thin films are subjected for systematic photocatalytic experiments on a model dye, Rhodamine B dye. It is also targeted to determine the formation of intermediates/reactive oxygen species (ROS) during the irradiation of the catalyst in aqueous condition. The authors are aware that these results with Rhodamine B may not be translated directly to the blood experiments; however, this study is regarded as important pilot-investigation to understand the photocatalytic behavior of the fabricated class of films and exploring their viability for their usage in the development of lung-assist biomedical device.

## 2. Experimental

### 2.1. Preparation of Ti doped indium tin oxide

Tin doped indium oxide (ITO) thin films have been prepared on cleaned quartz plates (size: 30 mm x 10 mm) by reactive DC magnetron sputtering technique. Initially,  $\sim 200$  nm thick tin doped indium oxide (ITO) thin films (from indium (90%) + tin (10%) metallic target) have been prepared. Then specific control thickness Ti layer have been made with  $\sim 50$ -90 nm thick Titanium containing thin film (from Ti metal target) coatings onto the ITO films. Both ITO and Ti films have been prepared at room temperature (300 K). Subsequently, the ITO-Ti stacks have been carefully annealed at  $873 \pm 5$  K for one hour in the ambient atmosphere and the annealing condition is one of the specific pathways to obtain the targeted property film and it helps diffusion and oxygen incorporation stages. As per the thickness of ITO and Ti, the film samples (catalysts) are named as  $C_1$ ,  $C_2$ ,  $C_3$  and  $C_4$  (Table 1). More details on the preparation method have been given in detail in our earlier literature.<sup>12</sup>

### 2.2. Characterisation of $\text{TiO}_2/\text{ITO}$

The resulting Ti doped indium tin oxide composite (Ti:ITO) have been characterized using XRD (Panalytical), Raman spectroscopy (Horiba Jobin Yvon, Lab Ram HR 800 with excitation wavelength 633 nm), optical absorption (double beam JASCO V-570 UV Vis spectrophotometer in the wavelength range 280 – 800 nm with a blank quartz plate as reference), thickness and refractive index (Filmetrics- F-20), Surface morphology (SEM), and the compositional analysis (by EDAX).

All the growth parameters and measurements have been ascertained to be repeatable and reproducible within the experimental limits.

### 2.3. Photocatalytic experiments

The photocatalytic efficiencies of the prepared catalysts were determined using aqueous Rhodamine B Dye (of different concentrations) with the irradiations of 254 nm incident light; the incident photon flux from the surface of the catalyst is measured by Thor Flux meter (calibrated). As it is well known that the photo-catalytic activity depends upon the (i) concentration of the dye molecules, (ii) pH, (iii) temperature, (iv) the incident wavelength, and (v) photon flux, and hence, experiments were designed suitably to extract the required information.

The dye concentration was taken as 5 ppm and the pH of the medium pH 6.5; the temperature is maintained at 300 K throughout the experiment. The degradation of the dye without the catalyst has been evaluated under nearly identical conditions. A 3.5 ml of the dye solution was taken in a quartz cuvette, and the catalyst was placed in the cuvette containing the dye solution and was irradiated perpendicularly to the surface of the films for the 5 hours under the UV light (6 watt) of wavelength 254 nm. The experiments were replicated to get consistent duplicate results within the limits of the acceptable errors.

## 3. Results and discussion

### 3.1. Interpretations of surface properties

Thickness of individual ITO and Ti in the prepared films and their refractive index values (at 632.8 nm) are summarised in Table 1.

**Table: 1** Optical properties of prepared Ti:ITO composite films

Sample Code	ITO Thickness t1, nm	n*	Ti Thicknes s t2, nm	n	Combined thickness (t1+t2), nm	Optical band gap, eV
$C_1$	234	2.05	36.17	2.49	270	3.77
$C_2$	188	2.12	77.21	2.43	265	3.75
$C_3$	120	2.14	63.66	2.47	183	3.72
$C_4$	190	2.14	70	2.44	260	3.75

\* where n is the refractive index obtained @632.8 nm.

It is difficult to measure the accurate thickness (and refractive index) of Ti:ITO (as these calculations involve a model system with known parameters; there is no model available for metal doping in ITO thin films). Though the individual thickness of ITO (120 nm to 230 nm) and Ti (37 nm to 77 nm) are varied the total thickness lies in between 180 nm to 270 nm. Samples labelled as  $C_1$  has highest thickness of ITO, and  $C_4$  (and  $C_2$ ) has high Ti; thus, the representative data for  $C_1$  and  $C_4$  are presented for SEM and EDX. It may be noted that whatever be the

thickness, the top layer of the catalyst is expected to have more Ti or may be its oxides. The refractive index (at 632.8 nm) of the Ti-ITO is seen almost constant at around 2.4, and the optical band gap values of the prepared films are in the range of 3.72-3.77 eV (as evaluated by optical spectrophotometry).

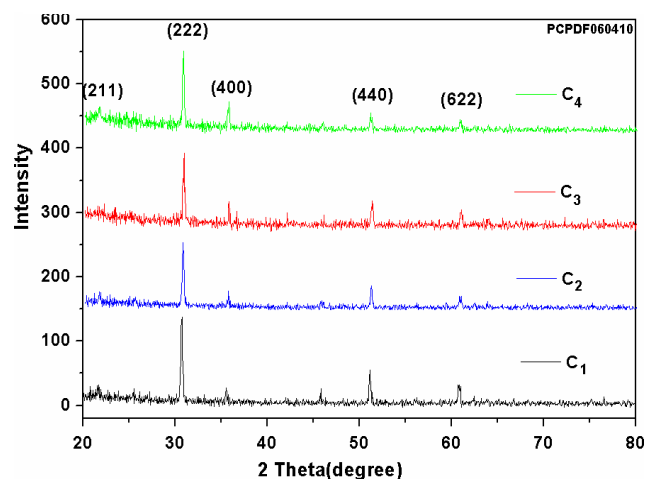


Fig. 1 X-ray diffraction pattern of the prepared catalysts

Fig.1 gives the X-ray diffraction pattern of these catalysts; they showed polycrystalline nature with oriented planes; the dominant plane being (222). From the JCPDS files (File no: PCPDF 060410) this material has found have similarities to  $\text{InTi}_2\text{O}_5$ . Since the characteristic peaks of  $\text{InTi}_2\text{O}_5$  coincides with that of  $\text{In}_2\text{O}_3$ . However, there are many points are to be considered to confirm the composition of the film. Hence, further characterisation techniques are adopted to understand the composition.

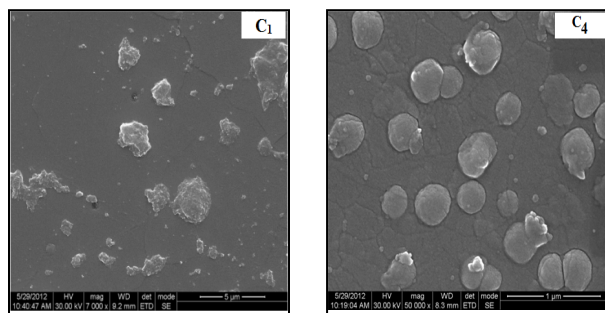


Fig. 2 SEM images of the catalysts (C1 and C4).

### 3.2 Composition of the prepared film catalysts

The EDX analyses (Fig. 3) reveal that the composition of the two prepared films  $C_1$  and  $C_4$  films, as In:22.25At%, Sn: 1.97 At%, Ti:5.23 At% and O:70.55 At%, and In:16.09At%, Sn: 1.50 At%, Ti:6.97 At% and O:75.43 At%, respectively. The typical surface morphology (Scanning Electron Micrographs) and the energy diffusion X-ray (EDX) characterization of the catalysts:  $C_1$  and  $C_4$  are presented in Fig. 2 and Fig 3, respectively. It may be noted that the surface of the films has micron sized islands, presumably the oxides of indium and the outermost layer of the catalyst is expected to have significant proportion of  $\text{TiO}_2$ . Results indicate, the film  $C_1$  has higher In:Ti ratio (i.e. 4.25) than the  $C_4$  (i.e. 2.31).

During the annealing, indium and tin might have been diffused into the titanium layer; the diffusing concentration of indium and tin vary significantly depending on the thickness of the Ti deposition. The film  $C_1$  has significantly higher intensity of reflections from 222; 400, 440 planes than that of the film  $C_4$  in XRD. It can be clearly corroborated with the above In:Ti ratio and the diffusion of Indium to the surface.

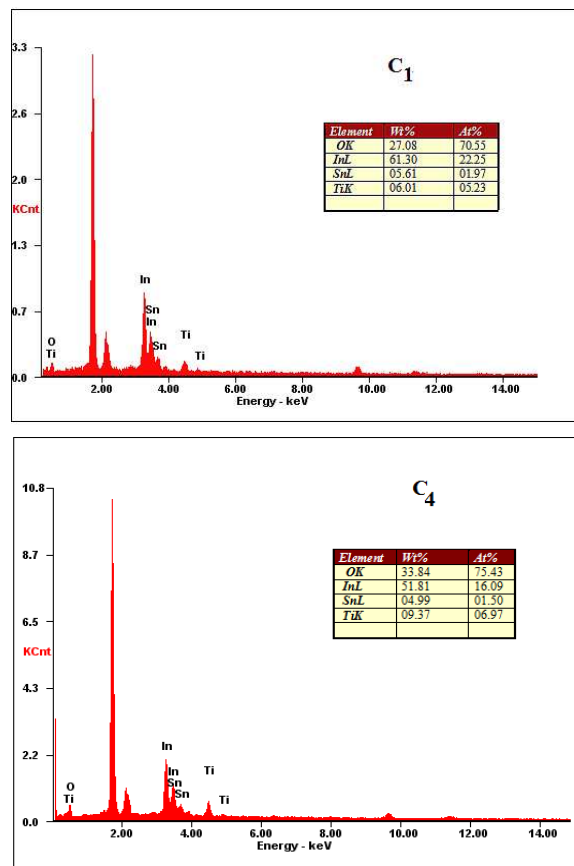


Fig. 3 EDX Profile of the representative films: Composition of  $C_1$  (in the top) and  $C_4$  (in the bottom)

Thus, the surface of the catalyst is expected to contain oxides of titanium, indium and tin. Interestingly, indium and tin though detected by EDX, does not show any Raman active bands.

The XRD profile exhibited predominant reflections at around  $32^\circ$  ( $2\theta$ ) from the (222) Plane, which are due to the characteristic orientation of planes ideally from the indium oxide material.<sup>20</sup> All the four films have moderately strong peaks at  $2\theta$ :  $36^\circ$  and  $52^\circ$  appeared, which are due to the reflections from 400 and 440 planes of Ti in Ti:ITO, respectively. The above peaks are matching to the cubic bixbyite structure of indium oxide.<sup>21</sup> It clearly ascertains that the doping of Ti on ITO matrix led to the same crystalline structure of indium oxide. Additionally, it can be noted that minor shifting of the peaks correspond to 400 and 440 plans clearly evident that some of the In(III) cations are substituted by the Ti(IV) ions in the  $\text{In}_2\text{O}_3$  crystal matrix.<sup>21</sup> Since, the ionic radii of In(III) and Ti(IV) are  $0.80 \text{ \AA}$  and  $0.61 \text{ \AA}$ , respectively. The substitution of ionic impurities in the lattice could be possible during the annealing process after the magnetron sputtering. Since, the content of Ti is less than 10 At%, the peak width broadening is very milder, and it can be



noticed on the reflections from 400 and 440 plans ( $C_3$  and  $C_4$ ). It can be considered to be a hint for partial phase separation and formation of  $TiO_2$  after the sputtering of the Ti over the ITO surface. Also the peaks correspond to 222; 400, and 440 are common to anatase phase of  $TiO_2$ . Hence, further Raman studies are carried out to verify the oxide formation.

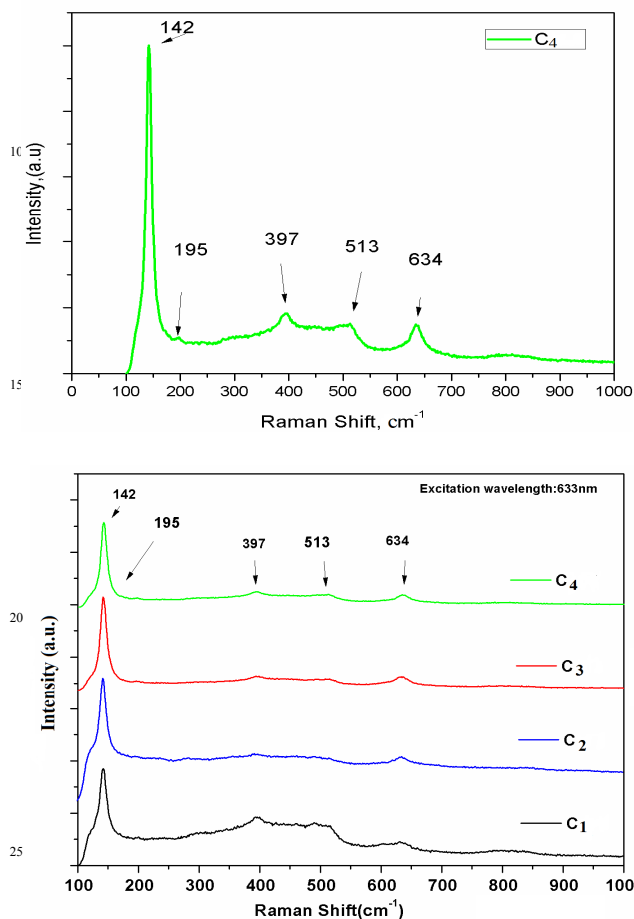


Fig. 4 Raman Spectra of the various composite films prepared (comparison in bottom) and for only  $C_4$  (in the top).

Fig. 4 shows Raman Spectra (excitation wavelength 632.8 nm) of the prepared composite films. In the spectra, the sample  $C_4$  has peaks at  $142\text{ cm}^{-1}$  (Eg),  $195\text{ cm}^{-1}$  (Eg),  $397\text{ cm}^{-1}$  (B1g),  $513\text{ cm}^{-1}$  (A1g) and  $634\text{ cm}^{-1}$  (Eg), which are in close agreement with the anatase phase of  $TiO_2$ . Ohsaka et al<sup>22</sup> reported on anatase single crystal such that six Raman active modes (A1g+2 B1g+3 Eg) are appeared at  $144\text{ cm}^{-1}$ ,  $197\text{ cm}^{-1}$ ,  $399\text{ cm}^{-1}$ ,  $513\text{ cm}^{-1}$ ,  $519\text{ cm}^{-1}$  and  $639\text{ cm}^{-1}$ . Interestingly, indium and tin though detected by EDX, does not seem to possess Raman active bonds.

From the EDX and Raman spectra, the composition of the films has been arrived as  $In_2O_3 \cdot xTiO_2$  (where  $x$  depends on the thickness of the Ti coating). The films  $C_1$  and  $C_4$  can be expressed as  $In_2O_3 \cdot \frac{1}{2}TiO_2$  and  $C_4\ In_2O_3 \cdot TiO_2$ , respectively. The anticipated (M:In):O ratio is 1:1.5, whereas the calculated ratio for the prepared films is 1:1.6. The slight excess of oxygen gives a surprise, as the annealing process could not favour the presence of -OH groups on the surface of  $TiO_2$ . Again, the formation of the  $TiO_2$  (as anatase form) is well corroborated with the earlier literature reports.<sup>19</sup> Hence, it should be noted that there could be a

possibility of adsorption of oxygen molecules on the surface of the prepared films.

XPS analysis exhibits peaks positioned at BE  $\sim 458.2$  and  $463.9\text{ eV}$  on the surface of the catalyst, which are characteristics of  $Ti\ 2p^{3/2}$  and  $Ti\ 2p^{1/2}$  in Fig. 5 (a). The peaks found in Fig. 5 (b) at BE  $\sim 444.2$  and  $551.7\text{ eV}$  are due to the presence of  $In\ 3d^{5/2}$  and  $In\ 3d^{3/2}$ , respectively<sup>23</sup>. Also, the occurrence of O 1s peaks can be confirmed by the signals at BE  $\sim 529.7$  and BE  $\sim 531.4\text{ eV}$ , which indicates that the Titanium and the Indium are exist in their oxide forms (Fig. 5 (d)). Since, the presence of indium oxide ( $In_2O_3$ ) can attribute the peaks at BE  $\sim 530\text{ eV}$ .<sup>24</sup> Moreover, the sputtering of Titanium on the ITO surface and annealing in oxygen environment might have contributed the formation of  $TiO_2$  apart from Ti-coating on ITO film surface (Fig. 5 (c)).

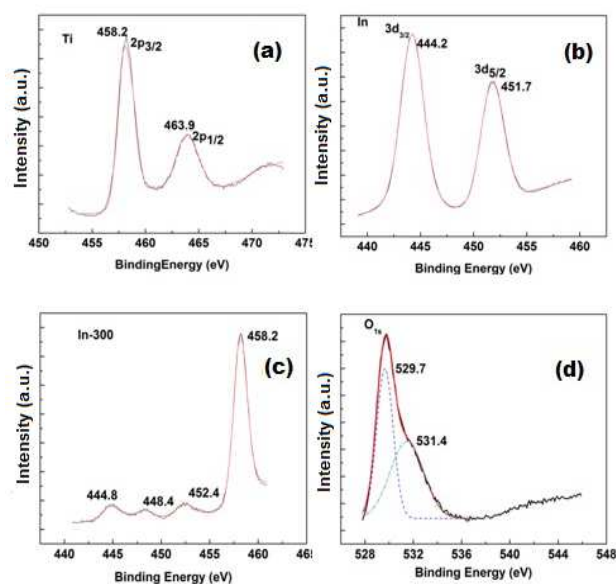


Fig. 5 XPS spectra of the composite films  $C_4$ .

### 3.3. Calculation of optical Band gap of the catalysts

The Figs 6 and 7 present respectively the optical transmission and the corresponding optical band gaps (as evaluated using Tauc relations for direct band gap) of the samples.

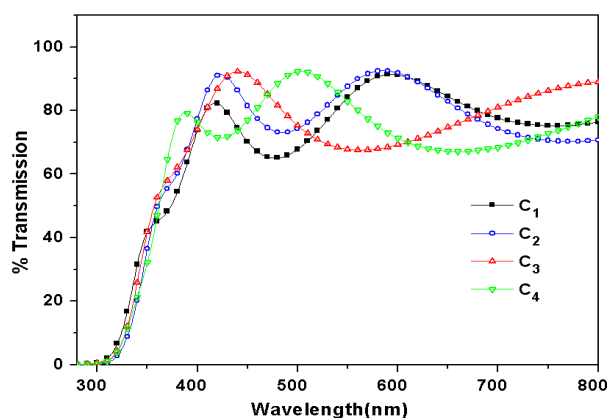


Fig. 6 Diffuse reflectance spectra of catalytic films ( $C_1$ - $C_4$ )

The Tauc relationship is expressed as

$$(\alpha h\nu) = \eta (h\nu - E_g)^n$$

Where  $\eta$  is a constant,  $E_g$  is the optical band gap and  $n$  is a constant which can take any values among 1/2, 3/2, 2 and 3 depending upon the type of optical transitions (direct or indirect),  $n = 1/2, 3/2, 2$  and  $3$  correspond to the direct allowed, direct forbidden, indirect allowed, and indirect forbidden transitions, respectively.<sup>253-27</sup>  $(\alpha h\nu)^{1/n}$  vs  $h\nu$  plot gives a linear relationship, and the intercept on the x axis gives the optical band gap. Table 1 summarizes the (direct,  $n = 2$ ) optical band gaps. The optical band gap of all the samples is  $\sim 3.7$  eV.

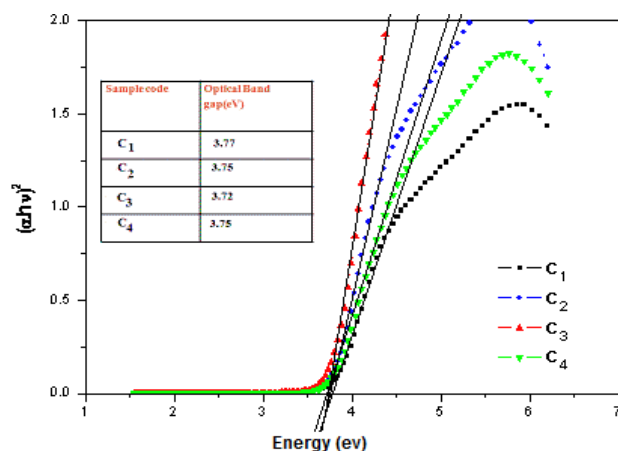


Fig. 7 Tauc plots for the band gap prediction from optical transmissions of prepared film catalysts.

This observed optical band gap value clearly indicates that the Ti loading of on ITO has increased the band gap energy than reported value for  $\text{In}_2\text{O}_3$  of 3.5 eV.<sup>21</sup>

### 3.4. Evaluating the photocatalytic efficiency

It is essential to understand the photocatalytic capacity of the prepared material before it can be employed in our target of lung assistive device purpose. Dye decolorization is a widely used tool to assess the first-hand information and capacity of any newly developed photocatalytic material. In general, Methylene Blue or Rhodamine B is used as a model system<sup>28-31</sup> to check the degradation efficiency of the prepared material under certain standard experimental conditions.<sup>31</sup>

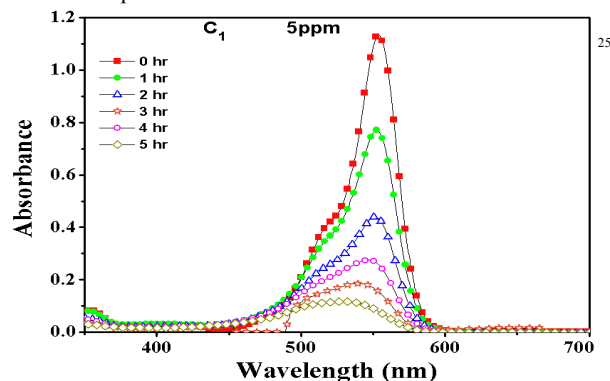


Fig. 8 Absorption spectrum for the photodegradation of Rhodamine B by TITO catalyst C1 under UV-light.

In this study, the photodegradation of the Rhodamine B was investigated using  $\text{Ti}/\text{TiO}_2$ -ITO films under UV irradiation (254 nm). It is anticipated that the 254 nm light can generate electron-hole pairs and the excess energy above the optical band gap

energy may be utilized in giving kinetic energy (KE) to the photo-generated charges. This additional KE may possess enough energy either to cross over or tunnel through the barrier at the interface (of the catalyst/ liquid). The experiments were repeated under various conditions to understand the involvement of different parameters in the photodegradation of dye.

To select the most effective photocatalytic system among the prepared catalysts (C<sub>1</sub>, C<sub>2</sub>, C<sub>3</sub> and C<sub>4</sub>), RhB degradation was investigated. In this case, the dye concentration was taken as 5 ppm and pH of the medium was adjusted with NaOH to arrive pH 6.5. A 3.5 ml of the dye solution was taken in a mini reaction vessel (quartz cuvette) and a particular film catalyst ( $3.0 \times 0.8 \text{ cm}^2$  dimension) was placed in the cuvette containing the dye solution. Then, the reaction system was placed in-front of the UV-light source (6 watts, 254 nm, in such a way that the film surface is perpendicular to the UV-light).

The distance between the UV source and the film was 5 cm. After each successive hour, the absorbance of the irradiated solution was recorded by using UV-1601 SHIMADZU spectrophotometer. The absorbance spectra of the dye solution irradiated in presence of TITO catalysts are provided in Fig. 8. The results clearly indicate that the peak at  $\lambda_{\text{max}}$  of 554 nm is gradually decreased with time, and the dye was almost degraded (90%) within five hours of irradiation. When a quartz plate was coated with titanium in our method, only  $\text{TiO}_2$  coated samples ( $\text{TiO}_2$ -alone) was obtained. The photodegradation of the  $\text{TiO}_2$ -alone film was found to be comparatively less than that of titanium doped ITO plate (sample C1). Results shown in Fig. 9 indicate that our titanium coating on ITO has given different kind of catalytic surface (characterized as In doped  $\text{TiO}_2$ ) than the  $\text{TiO}_2$  coating on quartz film.

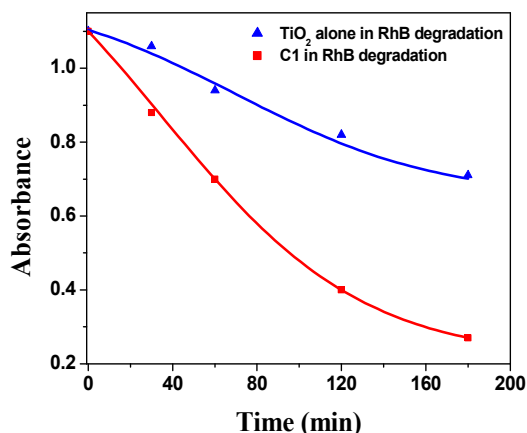


Fig. 9 Comparison of Rhodamine B degradation aided by  $\text{TiO}_2$  alone (blue line) and catalytic film C1 (red line) under various time intervals.

### 3.5. Kinetics of photodegradation

The detail of the kinetics of the degradation of the various catalysts has been shown in Fig. 10. The highest degradation efficiency was shown by catalyst C<sub>1</sub> (with 90% degradation) followed by the catalyst C<sub>3</sub> (87% degradation in five hours), and the degradation rate was much faster in case of the catalyst C<sub>1</sub>.

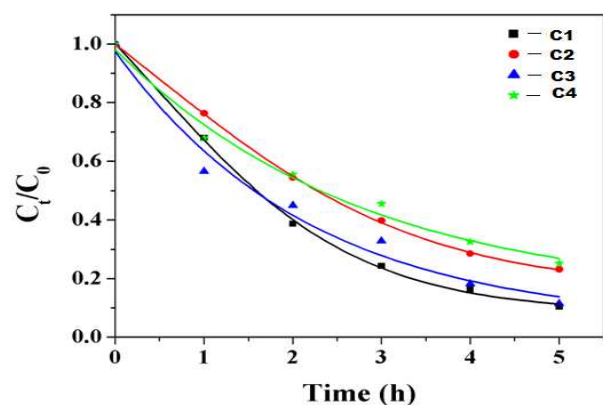


Fig. 10 Kinetics of photodegradation of RhB by various catalysts (C1, C2, C3 and C4).

When photodegradation reactions were performed without supplying oxygen (bubbling of oxygen) it is expected to slow down after certain time period. However, the photodegradation has increased with an increase of irradiation time. It confirms that the reaction is not subsiding with the exhaustion of dissolved oxygen. It is quite different from the normal observation one can find in any photo-oxidation process. Interestingly, the photooxidation is taken over due to the continuous formation of *in-situ* oxygen under the experimental conditions.

As the concentration of dye is an important parameter in the photodegradation, the effect of initial concentration of the dye was verified by keeping the other parameters constant in the photocatalytic experiments. The initial dye concentration in photocatalysis was varied from  $1 \times 10^{-5}$  to  $2 \times 10^{-5}$  mol L<sup>-1</sup>.

**Table 2.** Comparison of photodegradation rate constants of Rh B dye in different concentration by catalyst C<sub>1</sub> at pH 6.5

Dye Concentration		Rate constant (10 <sup>-3</sup> min <sup>-1</sup> )
(ppm)	(mol L <sup>-1</sup> )	
5.0 ppm	$1.0 \times 10^{-5}$ mol L <sup>-1</sup>	7.64
7.5 ppm	$1.5 \times 10^{-5}$ mol L <sup>-1</sup>	4.08
10.0 ppm	$2.0 \times 10^{-5}$ mol L <sup>-1</sup>	3.98

The degradation rates were evaluated from the linear relationship of  $\ln(C_0/C_t)$  versus time (Fig. 10). The rate constants were decreasing from  $7.64 \times 10^{-3}$  min<sup>-1</sup> to  $3.98 \times 10^{-3}$  min<sup>-1</sup> with an increase in initial concentration (Table 2).

### 3.6. Effect of dye concentration on the photodegradation

As the oxidation reaction occurs by the hydroxyl radical generated via surface bound hydroxyl groups, the competition of dye molecules at higher concentration results in the decrease of degradation rate (Fig. 11). In addition, at higher concentration, the light intensity reaching the TiO<sub>2</sub>/Ti-ITO thin film surface is reduced due to the lower solution transparency, increase in the quantity of intermediates and competing side reactions along with the dye decomposition.

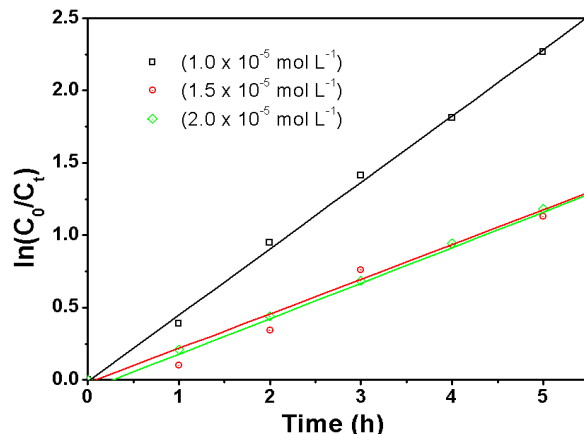


Fig. 11 Effect of dye (RhB) concentration on the photodegradation kinetics by the catalyst C<sub>1</sub>.

### 3.7. Formation of active oxygen species and effect of scavengers on the photodegradation

In general, the isopropanol is having high reactivity to react with hydroxyl radicals<sup>32</sup> and the control studies were carried out to verify the occurrence of hydroxyl radicals<sup>33,34</sup> in the present catalyst system under UV light. However, the isopropanol did not inhibit the dye degradation in the studied system. On the other hand, the isopropanol (1%) had decreased the photodegradation aided by the TiO<sub>2</sub>-alone film system, which could be following the hydroxyl radical mechanism.

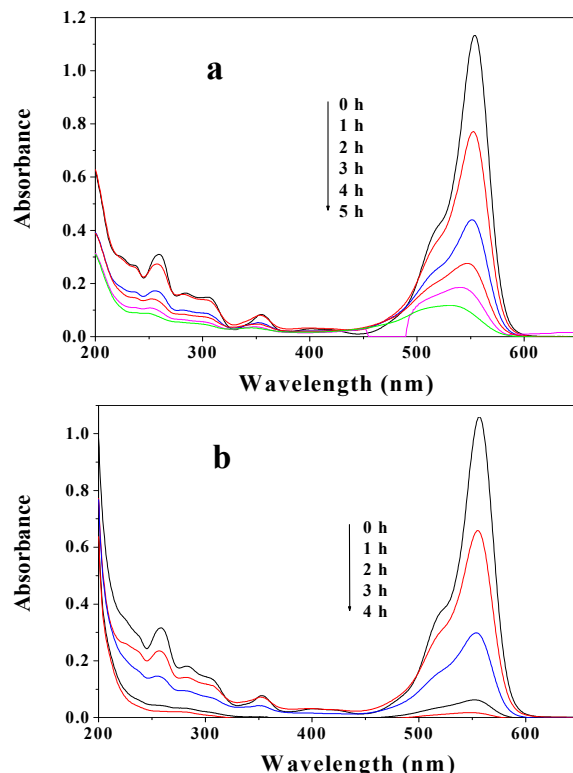


Fig. 12 a) Photodegradation of Rhodamine B by Catalyst C<sub>1</sub> in absence of isopropanol. b) in presence of isopropanol (1%) [C<sub>1</sub> and dye 5 ppm].

Results obtained from control study (Figure. 12 b)) reveal that the OH radicals are not the predominant species during the photocatalytic process by films C<sub>1</sub>. It was further clarified the

photocatalytic studies performed in DCM medium has also provided the identical trend of results (i.e. there was no inhibition of dye degradation). Consequently, we presumed that there could be some other oxygen species responsible for the dye degradation in the present system.

When the experiments were conducted in presence of benzoquinone, the degradation of the dye was suppressed significantly. Also, series of experiments were carried out to verify the linear relationship of the addition of benzoquinone, and the suppression of photocatalysis.<sup>35</sup> The dye degradation is decreasing directly with the increase in the concentration of benzoquinone (such as 10, 20 and 30 %). It is clearly indicating that the addition of benzoquinone is inhibiting the active oxygen species,<sup>35</sup> which is responsible for the dye degradation.

Further, kinetic studies were conducted to understand the irradiation time dependent response of the photodegradation in the presence of benzoquinone, and the results are presented in the figures (Fig.13). It indicates the formation of superoxide during the irradiation of the catalyst in the aqueous medium under UV irradiation. The competitive reactions of Rhodamine B and the benzoquinone were trailed under different time intervals. The control studies reveal that almost 65% of the photodegradation was suppressed by the benzoquinone (Fig.13 b). Hence, it is

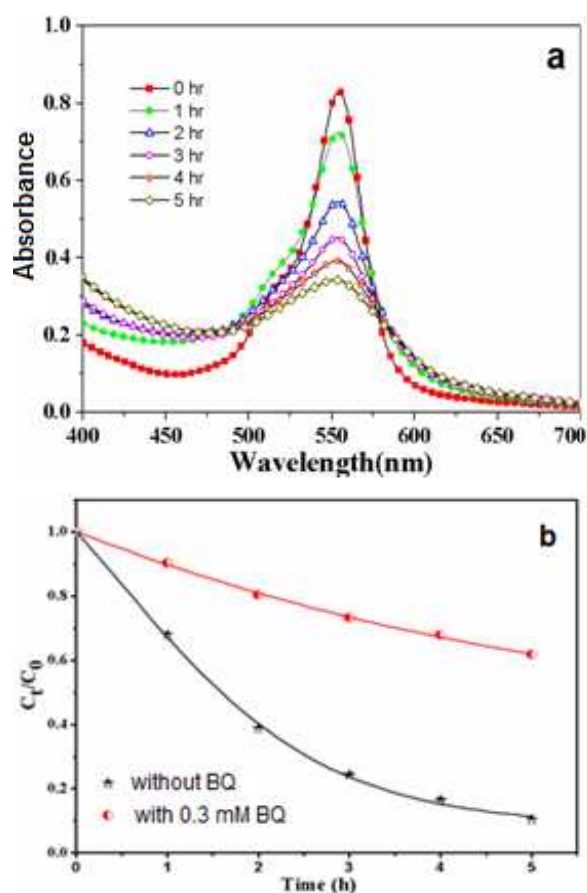


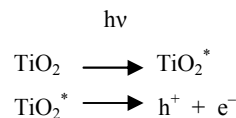
Fig. 13 Photodegradation of RhB by Cl: a) UV-visible absorption spectra of the degradation in presence of 30% benzoquinone b) Kinetics of the degradation with (30%) and without benzoquinone.

arrived that superoxide is forming under the photocatalytic conditions, and it is the key oxygen species responsible for the

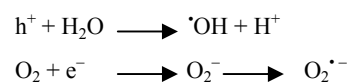
photodegradation of dye.

### 3.8. Plausible mechanism of photocatalysis

Generally, the TiO<sub>2</sub> based films (TiO<sub>2</sub>-ITO) catalyst in aqueous solution can produce the electron-hole pair under the UV irradiation, which can be expressed by the following intermediate steps.<sup>36,37</sup>



When the photogenerated electron (e<sup>-</sup>)-hole (h<sup>+</sup>) pair migrates over the surface of the TiO<sub>2</sub>/Ti-ITO film, there were two reaction route possible: the hole can interact with surface bound molecules (water or dye); electrons were captured by oxygen molecules adsorbed on the film surface to give superoxide radicals.<sup>6,37,38,39</sup>



Here, the isopropanol studies were conducted to discriminate the role of hydroxyl radical and direct hole (h<sup>+</sup>) oxidation of dye. The results obtained clearly infer that the scavenger isopropanol was not inhibiting the degradation process and it is presented in Figure 11a. Hence, the hydroxyl radicals are not the main species responsible for the photodegradation.

Usually, the main reason of the loss of efficiency of TiO<sub>2</sub> photocatalyst is noted because of recombination process. Since, the duration required for the quenching of photogenerated electrons with surface molecules is of almost similar order. According to Carmalt et al.<sup>37</sup> the composite films have different probabilities like shuttling of electrons from conduction band of TiO<sub>2</sub> to conduction band of another metal oxide. In this case we have TiO<sub>2</sub> to In<sub>2</sub>O<sub>3</sub>, whereby prevent the recombination process. Since we propose exchange of Ti<sup>4+</sup> within some of the In<sup>3+</sup> positions have different mechanism than the pure In<sub>2</sub>O<sub>3</sub> sites. Actually, the pure In<sub>2</sub>O<sub>3</sub> sites are responsible for the production of superoxide ions from the shuttled electrons. Additionally the impure In<sub>2</sub>O<sub>3</sub> system is serving as oxygen absorber due to material property. Additionally, the TiO<sub>2</sub> suppose to act as hole scavenger or retain the holes for photooxidation process. However, there is no evidence of hole aided mechanism (hydroxyl radical route) and the holes are also not stable in TiO<sub>2</sub> due to the unsuitable pH conditions. Overall, selectively superoxide is produced along with rapid mobility of the oxygen in the aqueous system from the composite surface under irradiation.

As a result, the superoxide radicals facilitating the degradation of dye process slowly.<sup>38,40</sup> Further, the benzoquinone study suggests that superoxide formation is the main cause for dye degradation (Fig. 13 b). The formation of superoxide along with subsequent photodegradation for long duration is only possible, if the system has self-sustained oxygen supply during the irradiation. It could be possible due to the property of the prepared film catalyst to generate oxygen in the aqueous medium under UV irradiation by either water splitting or absorbing dissolved oxygen.<sup>40</sup> The superoxide ions under acidic medium



can generate  $\text{HO}_2^\cdot$  radicals. These species can evolve oxygen either via formation of hydrogen peroxide or by reaction with superoxide species in acidic condition. Therefore, it is proposed that the prepared  $\text{TiO}_2/\text{Ti-ITO}$  catalyst can *in-situ* generate oxygen molecules.

Photodegradation experiments conducted by controlling dissolved oxygen (DO) revealed that increase of the dissolved oxygen had offered enhancement in dye degradation<sup>41</sup>. However, the influence of the DO have resulted in the enhancement of the degradation upto the initial 1-2 h duration (Supplementary information Fig. S17). Interestingly, the results obtained for the dye solution bubbled with  $\text{N}_2$  gas, and the solution with controlled DO ( $3.9 \pm 0.2$  ppm) have been found to be almost similar, whereas the solution with higher (two fold) DO values ( $9.5 \pm 0.2$  ppm) showed a slight increase in the degradation at the initial period, and then it becomes similar to moderate DO condition in 2-3 h (Fig. 15). Further, the aqueous solutions after dye degradation were identified to have the DO values in the range of 5.5 - 7.2 ppm, which can substantiate the *in-situ* oxygen generation during the photocatalysis. Moreover, we assume that the identified value could be nothing but the balance of oxygen in solution after the consumption of oxygen during the dye degradation/superoxide formation.

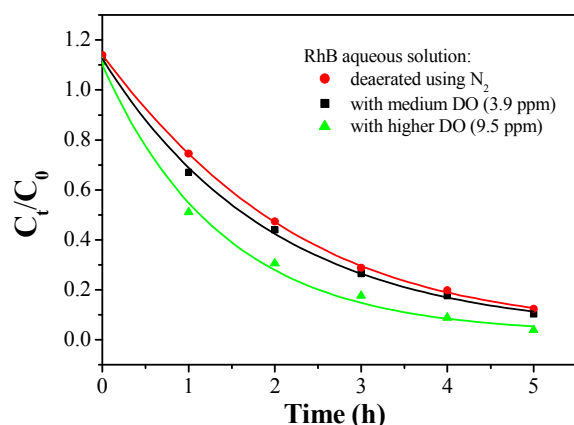


Fig. 14. Effect of dissolved oxygen on the kinetic of Rhodamine B photodegradation.

Here, the prepared film is distinguishing itself from the conventional  $\text{TiO}_2$  films, which are known for the formation of hydroxyl radicals<sup>37</sup> and hence, they could not be favourable to the blood samples for oxygenation purposes. On the other hand, our prepared film has capacity to generate oxygen, which could be a special property exerted by the controlled thickness coating of Titanium (also the combination of  $\text{TiO}_2/\text{Ti}$ ) on the ITO surface. There are two advantages in the controlled thickness of Ti over ITO, i.e., i) the opportunity for incorporation of Ti<sup>4+</sup> on the  $\text{In}^{3+}$  lattices and the ii) formation of hybrid nanocomposite  $\text{TiO}_2/\text{Ti-ITO}$ , which serve as oxygen shuttling platform and facilitates the formation of superoxide selectively.

Further, it can be explained with the help of the most widely accepted theory of metal oxide semiconductor gas sensing.<sup>42</sup> It states that “when a metal oxide semiconductor gas sensor is exposed to air, oxygen is adsorbed on its surface and go on to be

ionized by electrons from its conduction band and it will form species such as  $\text{O}_2^{\cdot-}$ .”<sup>42</sup> The same phenomenon is applicable to our metal oxide thin film systems also. Here, the adsorbed oxygen is mobilized in solution during the reduction some of the oxygen molecules by the conduction band electrons. Once, the reduced species moves away further molecules of oxygen will be captured by the film from the aqueous/air environment. In normal condition, the reduction process by the semiconductor will go sluggish after a certain period. However, our system is clubbed with photocatalytic process and hence, the electron excitation to conduction band occur to produce superoxide radicals. Hence, the oxygen generation/superoxide can be complemented by the aid of photocatalysis on the films. The above process can be continuously carried out for the long time with the help of irradiation. Once the irradiation is switched off, then the superoxide formation is stopped.

Already we observed that the addition of isopropanol was not decreased the photodegradation of the dye (Figure 12 b) and surprisingly it has offered opposite effect, i.e., enhancement of the dye degradation. Accordingly to our hypothesis, the reduction of oxygen is the process helps more mobility of oxygen in the reaction medium and here, the isopropanol is acting as a donor of electron to the conduction band of the composite film. Consequently, the degradation process was accelerated upon addition of isopropanol by synergism with photo-assisted electron transfer. This result is a support to strengthen our proposal of oxygen radical mobility versus photodegradation.

To our best knowledge, only few reports are available in literature for the preparation of  $\text{TiO}_2\text{-ITO}$  or  $\text{Ti:ITO}$  films, which were made for different application.<sup>20,21</sup> Hence, it can be considered as the first time report about the hybrid composite film ( $\text{TiO}_2\text{-Ti-ITO}$ ) for its selective photocatalytic oxygen generation process. The results of the present study gave understanding about our prepared composite films to be a genuine material, which is first of its kind in the development of artificial lung assistive device. Further, more advance studies will be required to explore the utilization of this property for other useful applications.

When photocatalytic studies were carried out with real blood samples in a quartz tube internally coated with  $\text{TiO}_2/\text{Ti-ITO}$ , the oxygen concentration was found to be increased. The enrichment of oxygen was monitored using online medical diagnostic device (heme- $\text{O}_2$  detection device). Though this study has arrived to the qualitative information about the superoxide formation under photocatalytic condition, a detailed study would be necessary to evaluate the quantitative measure of superoxide/oxygen intermediates generated by photocatalysis. Also a dedicated investigation on the blood samples as per the medicinal science protocols is under progress using the prepared composite films.

### 3.9. Reusability of the film catalysts

Reusable study on the photodegradation of RhB by catalyst  $\text{C}_1$  reveals that the catalytic film is having significant reusability, and the performances on the twelve consecutive cycles were almost similar as given in Figure 15. However, the repeatability cycles were performed after giving a resting time of 8-10 hours between each cycle, which may be helping equilibration of electron hole-  
reset to bring the material to its original condition.

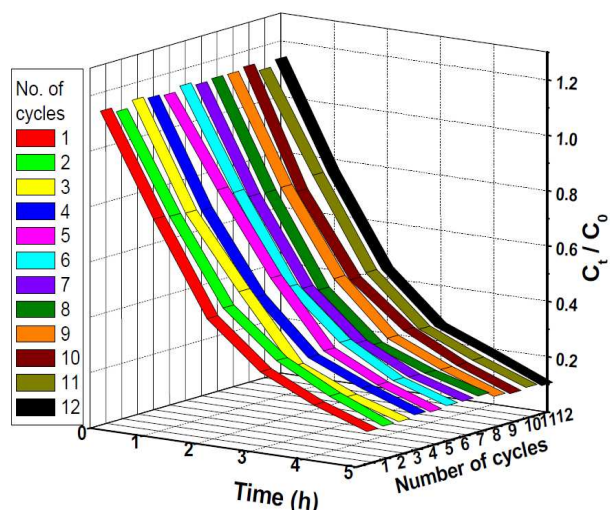


Fig. 15. Kinetic plots of recycle studies on the photodegradation of RhB by ITO Catalyst C<sub>1</sub>.

Upon repeated usage of 60-80 times, there is a slight decrease in the catalytic efficiency (5-8% decrease), which could be due to the surface scratches or mechanical abrasions during the handling and cleaning. Overall, the prepared catalytic films are found to be one of the genuine classes of materials, which need further investigations for better exploitation in various applied fields.

#### 4.0. Conclusions

The TiO<sub>2</sub>/Ti-ITO catalytic films are found to be efficient in the photooxidation of Rhodamine B and the effective photocatalysis of dye was achieved with the catalyst C<sub>1</sub> (RhB 5 ppm, at pH 6.5) in 5 hours irradiation using 254 nm UV lamp. The process follows the pseudo-first order kinetics, slow in nature, and the superoxide is generated as the main species by the composite films responsible for the photodegradation of Rhodamine B dye.

The interesting feature of these composite films is its photocatalytic behaviour, i.e. it does not produce the hydroxyl radicals. The electron donor reagents have positive effect on the photodegradation process and oxygen generation. Further, the composite films are reusable and continuously generating molecular oxygen during photocatalysis. These genuine characters are attractive and helpful to employ the TiO<sub>2</sub>/Ti-ITO films for photo-assisted bio-medical applications, including blood oxygenation. Since, it does not cause damage or cleave to the heme group due to the absence of hydroxyl radicals under irradiation. Further studies are needed to control the mechanistic pathways of these thin-films, which would offer a variety of applications from the prepared TiO<sub>2</sub>/Ti-ITO hybrid thin films.

#### Acknowledgement

The authors thank the Department of Chemistry, Indian Institute of Technology, Kharagpur, and Department of Physics, Indian Institute of Technology, Madras for various facilities and support.

#### Notes and references

a. Department of Physics, IIT Madras, Chennai 600036, India

b. Department of Chemistry, IIT Kharagpur, 721302, India

c. Apollo Hospital, Greams Road, Chennai 600006, India

d. National Institute of Technology, Suratkal, 575025 Karnataka, India

e. The National Institute of Engineering, Mysore, 570008, India

\*Department of Chemistry, Green Environmental Materials & Analytical Chemistry Laboratory, Indian Institute of Technology, Kharagpur, 721 302, India. Fax: (+91) 3222-255303; Tel: (+91) 3222-282322; E-mail: raja.iitchem@yahoo.com

† Electronic Supplementary Information (ESI) available: Experimental procedure, results of preliminary studies and additional information about control studies.

- J. Gao, Q. S. Li, H. B. Zhao, L. S. Li, C. L. Liu, Q. H. Gong and L. Qi, *Chem. Mater.*, 2008, **20**, 6263.
- Q. Tian, M. Tang, Y. Sun, R. Zou, Z. Chen, M. Zhu, S. Yang, J. Wang, J. Wang and J. Hu, *Adv. Mater.*, 2011, **23**, 3542.
- M. Zhou, R. Zhang, M. Huang, W. Lu, S. Song, *J. Am. Chem. Soc.*, 2010, **132**, 15351.
- G. K. Mor, O. K. Varghese, M. Paulose, K. Shankar, and C. Grimes, *Solar Energy Mater. Solar Cells*, 2006, **90**, 2011.
- M. A. Fox, M. T. Dulay, *Chem. Rev.*, 1993, **93**, 341.
- M. R. Hoffmann, S. T. Martin, W. Choi and D. W. Bahnemann, *Chem. Rev.*, 1995, **95**, 69.
- A. Mills and S. Le Hunte, *J. Photochem. Photobiol. A*, 1997, **108**, 1.
- C. Santato, M. Odziemkowski, M. Ulmann and J. Augustynski, *J. Am. Chem. Soc.*, 2001, **123**, 10639.
- J. M. Herrmann, C. Gullard, J. Disdier, C. Lehaut, S. Malato and J. Blanco, *Appl. Catal. B: Environ.*, 2002, **35**, 281.
- U. Bali, E. Çatalkaya and F. Sengul, *J. Hazard. Mater.*, 2004, **114**, 159.
- A. Aleboye, Y. Moussa and H. Aleboye, *Dyes Pigments*, 2005, **66**, 129.
- G. Sermin and O.Y. Özlem, *Chem. Eng. J.*, 2009, **155**, 684.
- T. Sano, N. Negishi, K. Koike, K. Takeuchi and S. Matusuzawa, *J. Mater. Chem.*, 1994, **4**, 380.
- J. A. Cowan, *Inorganic Biochemistry – An Introduction*, Ed. II, Wiley-VCH, Inc. Weinheim, 2013, pp 168-170.
- A. Subrahmanyam, T. Arockia Doss and T. Paul Ramesh, *Artificial Organs*, 2007, **31**, 819.
- A. Subrahmanyam, T. P. J. Ramesh and N. Ramakrishnan, *ASAIO J.*, 2007, **53**, 434.
- M. Addamo, V. Augugliaro, A. Di Paola, E. Garcia-Lopez, V. Loddo, G. Marci, R. Molinari, L. Palmisano and M. Schiavello, *J. Phys. Chem. B*, 2004, **108**, 3303; V. Pore, M. Ritala, M. Leskela, S. Areva, M. Järne and J. Järnström, *J. Mater. Chem.*, 2007, **17**, 1361.
- X. Yang, F. Ma, K. Li, Y. Guo, J. Hu, W. Li, M. Huo, and Y. Guo, *J. Hazard. Mater.*, 2009, **175**, 429.
- K. Kumar, R.N. Jagadeesh, R. Chandra and A. Subrahmanyam, *Appl. Surf. Sci.*, 2011, **257**, 3075.
- J. Kim, K. H. Ji, M. Jang, H. Yang, R. Choi, and J. K. Jeong, *ACS Appl. Mater. Interfaces* 2011, **3**, 2522.
- L. G. Bloor, J. Manzi, R. Binions, I. P. Parkin, D. Pugh, A. Afonja, C. S. Blackman, S. Sathasivam, and C. J. Carmalt, *Chem. Mater.* 2012, **24**, 2864.
- T. Ohsaka, F. Izumi, and Y. Fujiki, *J. Raman Spect.*, 1978, **7**, 321.
- P.V. Galiy and A.V. Musayanovych, *Funct. Mater.*, 2005, **12**, 457.
- C Sanz, C Guill'en and J Herrero, *Semicond. Sci. Technol.*, 2013, **28**, 015004.
- Santra K, Sarkar C K, Mukherjee and Ghosh B 1992 *Thin Solid Films* **213** 226.
- F. Wooten, *Optical Properties of Solids*, Academic Press, New York (1972).
- K. Kubota, Y. Kobayashi, K. Fujimoto, *Appl. Phys.* 1989, **66**, 2984.
- K. Ogura, S. Kurakami and K. Senoo, *J. Inorg. Nucl. Chem.*, 1981, **43**, 1243.
- T. M. Florence, *J. Electroanal. Chem.*, 1974, **52**, 115.
- A. Mills and J. Wang, *J. Photochem. Photobiol. A: Chem.*, 1999, **127**, 123.

- 
- 31 N. T. Dung, N. V. Khoa and J.M. Herrmann, *Int. J. Photoenergy*,  
2005, **7**, 11.
- 32 S. Gazi and R. Ananthakrishnan, *J. Hazard. Mater.*, 2010, **183**, 894.
- 33 Y. Anjaneyulu, N.S. Chary and S.S.D. Raj, *Rev. Environ. Sci*  
5 *Biotechnol.*, 2005, **4**, 245–273.
- 34 Patrick Mazellier and Michèle Bolte, *J. Photochem. Photobiol. A:*  
*Chem.*, 2000, **132**, 129.
- 35 R. Ananthakrishnan and S. Gazi, *Catal. Sci. Technol.*, 2012, **2**, 1463.
- 36 K. Ikeda, H. Sakai, R. Baba, K. Hashimoto and A. Fujishima, *J.*  
10 *Phys. Chem.*, 1997, **B 101**, 2617.
- 37 S. Ponja, S. Sathasivam, N. Chadwick, A. Kafizas, S. M. Bawaked,  
A.Y. Obaid, S. Al-Thabaiti, S. Basahel, I.P. Parkina and C. J.  
Carmalt, *J. Mater. Chem. A*, 2013, **1**, 6271
- 38 L. Zhang Y. Wang, T. Xu, S. Zhu and Y. Zhu, *J. Mole. Catal. A:*  
15 *Chem.*, 2010, **331**, 7.
- 39 G. Yang, Z. Jiang, H. Shi, T. Xiao and Z. Yan, *J. Mater. Chem.*,  
2010, **20**, 5301.
- 40 J. Shang, S. Xie, T. Zhu and J. Li, *Environ. Sci. Technol.*, 2007, **41**,  
7876.
- 20 41 H.-C. Liang, X.-Z. Li, Y.-H. Yang, K.-H. Sze, *Chemosphere*, 2008,  
**73**, 805.
- 42 N. Barsan, U.J. Weimar, *J. Electroceramics*, 2001, **7**, 143.